

Exclusive photoproduction of quarkonium at the LHC energies within the color dipole approach

Maria Beatriz Gay Ducati

Universidade Federal do Rio Grande do Sul.

Instituto de Física.

Grupo de Fenomenologia de Partículas de Altas Energias.

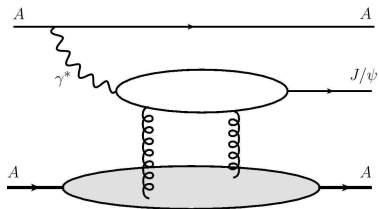
www.if.ufrgs.br/gfpae



- Introduction
 - Exclusive vector meson photoproduction
 - Pomeron exchange
 - Dipole formalism
 - Node effect
- Vector mesons production in pp and PbPb collisions
 - Differential cross section calculation
 - Vector mesons wave function
 - Dipole cross section model
- Results for J/ψ , ψ' and Υ production
 - Rapidity distribution of J/ψ and ψ'
 - Rapidity distribution of Υ production
- Summary

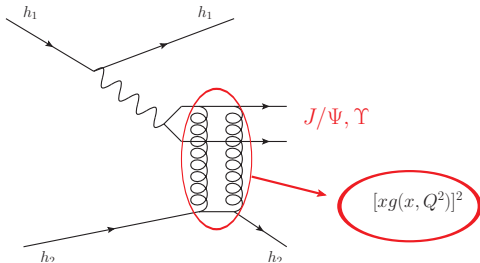
Exclusive vector meson photoproduction

- $\gamma + p \rightarrow V + p \rightarrow$ has been investigated experimentally and theoretically as it allows to test perturbative Quantum Chromodynamics
- The quarkonium masses (m_c, m_b), give a perturbative scale for the problem even at $Q^2 = 0$



Pomeron Exchange

- An outstanding feature of diffractive photoproduction of mesons in the high energy regime is the possibility to investigate the Pomeron exchange

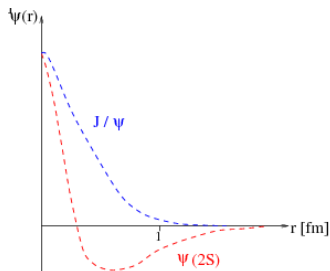


Pomeron \rightarrow two gluons (vacuum quantum numbers)

Node Effect

- The diffractive production of the 2S radially excited vector mesons, like $\Psi(2S)$, is specially interesting due to the node effect ¹

Node Effect: Strong cancellation of dipole size contributions to the production amplitude from the region above and below the node position in the 2S radial wavefunction.

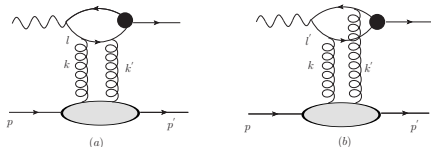


→ This is the origin of the large suppression of the photoproduction of radially excited vector mesons 2S versus 1S

¹J. Nemchik, N. N. Nikolaev, E. Predazzi and B. G. Zakharov, Phys. Lett. B 374, 199, 1996

Diffractive production of meson at $t = 0$

An important class of diffractive reactions where we can use a perturbative treatment is the vector meson production in DDIS: $\gamma^* p \rightarrow Vp$. Two gluons exchange diagrams that contribute to the amplitude of the vector meson leptonproduction are shown in the figure below:



In the color dipole formalism, the amplitude can be written as:

$$A \propto \Psi^\gamma \otimes \sigma^{q\bar{q}} \otimes \Psi^V, \quad (1)$$

Amplitude ²:

$$A_T(W^2, t = 0) = -4\pi^2 i\alpha_s W^2 \int \frac{dk^2}{k^4} \left(\frac{1}{l^2 - m_c^2} - \frac{1}{l'^2 - m_c^2} \right) \times f(x, k^2) e_c g_\Psi M_\Psi \quad (2)$$

$l(l')$ \rightarrow quark (antiquark) momentum

k \rightarrow gluons transverse momentum

$f(x, k^2)$ \rightarrow unintegrated gluons distribution.

The cross section is given by:

$$\frac{d\sigma_T^{\gamma^{(*)}p \rightarrow \Psi p}}{dt} = \frac{1}{16\pi W^4} |A_T|^2. \quad (3)$$

The constant g_Ψ can be determined from the decay $\Gamma_{e^+e^-}^\Psi$: $e_c^2 g_\Psi^2 = \frac{\Gamma_{e^+e^-}^\Psi}{12\alpha_{em}}$

²M. G. Ryskin, Z. Phys. C 57, 89, 1993

In the $\ln \tilde{Q}^2$ dominant approach, the amplitude is written as ²:

$$A_T \simeq 2\pi^2 i e_c g_\Psi M_\Psi \alpha_s(\tilde{Q}^2) W^2 \frac{xg(x, \tilde{Q}^2)}{\tilde{Q}^4} \quad (4)$$

and the transverse cross section is:

$$\left. \frac{d\sigma_T^{\gamma^{(*)}p \rightarrow \Psi p}}{dt} \right|_{t=0} = \frac{16\Gamma_{e^+e^-}^\Psi M_\Psi^3 \pi^3}{3\alpha_{em}(Q^2 + M_\Psi^2)^4} \left[\alpha_s(\tilde{Q}^2) xg(x, \tilde{Q}^2) \right]^2. \quad (5)$$

In \tilde{Q}^2 approach \rightarrow the amplitude is driven by two gluons exchange diagrams

$xg(x, \tilde{Q}^2) \rightarrow$ gluons distribution

The complete differential cross section (T+L) in the $\ln \tilde{Q}^2$ dominant is ²:

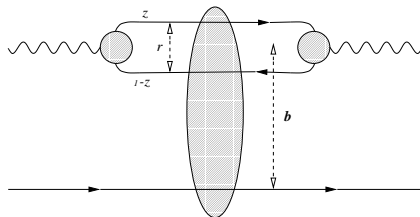
$$\left. \frac{d\sigma^{\gamma^{(*)}p \rightarrow Vp}}{dt} \right|_{t=0} = \frac{16\Gamma_{e^+e^-}^V M_\Psi^3 \pi^3}{3\alpha_{em}(Q^2 + M_V^2)^4} \left[\alpha_s(\tilde{Q}^2) xg(x, \tilde{Q}^2) \right]^2 \left(1 + \frac{Q^2}{M_V^2} \right)$$

$xg(x, \tilde{Q}^2) \rightarrow$ grows in small- $x \rightarrow$ undetermined

Dipole formalism \rightarrow can restrict $xg(x, \tilde{Q}^2) \rightarrow$ includes gluon saturation

Dipole Formalism

- In the LHC energy domain hadrons and photons can be considered as color dipoles in the light cone representation ³.
- The scattering process is characterized by the color dipole cross section representing the interaction of those color dipoles with the target.



r → dipole separation.

$z(1 - z)$ → quark(antiquark) momentum fraction.

b → impact parameter.

³ Nikolaev and Zakharov, Z. Phys. C 49, 607, 1991

Quarkonium production in pp collisions

The rapidity distribution for quarkonium photoproduction is given by

$$\frac{d\sigma}{dy}(pp \rightarrow p \otimes \psi \otimes p) = S_{\text{gap}}^2 \left[\omega \frac{dN_\gamma}{d\omega} \sigma(\gamma p \rightarrow \psi(nS) + p) + (y \rightarrow -y) \right], \quad (6)$$

Photon flux: ⁴

$$\frac{dN_\gamma(\omega)}{d\omega} = \frac{\alpha_{em}}{2\pi\omega} \left[1 + \left(1 - \frac{2\omega}{\sqrt{s}} \right)^2 \right] \times \left(\ln \xi - \frac{11}{6} + \frac{3}{\xi} - \frac{3}{2\xi^2} + \frac{1}{3\xi^3} \right), \quad (7)$$

$\omega \rightarrow$ photon energy

$S_{\text{gap}}^2 = 0.8^5 \rightarrow$ represents the absorptive corrections due to spectator interactions between the two hadrons ⁶

⁴ C. A. Bertulani, S. R. Klein and J. Nystrand, *Ann. Rev. Nucl. Part. Sci.* 55, 271, 2005

⁵ W. Schafer and A. Szczurek, *Phys. Rev. D* 76, 094014, 2007

⁶ A. D. Martin, M. G. Ryskin and V. A. Khoze, *Phys. Rev. D* 56, 5867, 1997. E. Gotsman, E. M. Levin and U. Maor, *Phys. Lett. B* 309, 199, 1993.

$$\sigma_{\gamma^* p \rightarrow V p}(s, Q^2) = \frac{1}{16\pi B_V} |\mathcal{A}(x, Q^2, \Delta = 0)|^2, \quad (8)$$

where the amplitude is ⁷

$$\mathcal{A}(x, Q^2, \Delta) = \sum_{h, \bar{h}} \int dz d^2 \Psi_{h, \bar{h}}^\gamma \mathcal{A}_{q\bar{q}}(x, r, \Delta) \Psi_{h, \bar{h}}^{V*}, \quad (9)$$

$B_V(W_{\gamma p}) = b_{el}^V + 2\alpha' \log\left(\frac{W_{\gamma p}}{W_0}\right)^2 \rightarrow$ diffractive slope parameter

$$\alpha' = 0.25 \text{ GeV}^{-2}$$

$$W_0 = 95 \text{ GeV}$$

$$b_{el}^{\psi(1S)} = 4.99 \pm 0.41 \text{ GeV}^{-2} \text{ and } b_{el}^{\psi(2S)} = 4.31 \pm 0.73 \text{ GeV}^{-2}$$

⁷ N. N. Nikolaev, B. G. Zakharov, Phys. Lett. B 332, 184, 1994

The light cone wave functions of the meson are written as:

$$\Psi_{h,\bar{h}}^{V,L}(r,z) = \sqrt{\frac{N_c}{4\pi}} \delta_{h,-\bar{h}} \frac{1}{M_V z(1-z)} \times [z(1-z)M_V^2 + \delta(m_f^2 - \nabla_r^2)] \phi_L(r,z)$$

$$\nabla_r^2 = (1/r)\partial_r + \partial_r^2$$

$$\begin{aligned} \Psi_{h,\bar{h}}^{V,T(\gamma=\pm)}(r,z) = & \pm \sqrt{\frac{N_c}{4\pi}} \frac{\sqrt{2}}{z(1-z)} \{ie^{\pm i\theta_r} [z\delta_{h\pm,\bar{h}\mp} - (1-z)\delta_{h\mp,\bar{h}\pm}] \partial_r \\ & + m_f \delta_{h\pm,\bar{h}\mp} \} \phi_T(r,z) \end{aligned}$$

$\Psi(1S)$: 8

$$\phi_\lambda(r, z) = N_\lambda \left[4z(1-z)\sqrt{2\pi R^2} \exp\left(-\frac{m_f^2 R^2}{8z(1-z)}\right) \exp\left(-\frac{2z(1-z)r^2}{R^2}\right) \times \exp\left(\frac{m_f^2 R^2}{2}\right) \right]$$

$\Psi(2S)$: 1

$$\phi_{2S}(r, z) = \phi_{1S}(r, z)[1 + \alpha_{2S}g_{2S}(r, z)]$$

$$g_{2S}(r, z) = 2 - m_f^2 R_{2S}^2 + \frac{m_f^2 R_{2S}^2}{4z(1-z)} - \frac{4z(1-z)r^2}{R_{2S}^2}$$

→ Boosted Gaussian Wavefunction (BG)

$N_\lambda, R, \alpha_{2S}$ → parameters from the orthogonality condition of wave functions

⁸ J. R. Forshaw, R. Sandapen and G. Shaw, JHEP 0611, 025, 2006

The GBW (Golec-Biernat and Wusthoff) parametrization is given by: ⁹

$$\sigma_{dip}(x, \vec{r}; \gamma) = \sigma_0 \left[1 - \exp \left(-\frac{r^2 Q_{sat}^2}{4} \right)^{\gamma_{eff}} \right],$$

$$\gamma_{eff} = 1$$

Saturation scale $\rightarrow Q_{sat}^2(x) = \left(\frac{x_0}{x}\right)^\lambda$

$x_0, \sigma_0, \lambda \rightarrow$ fitted to DIS HERA data

⁹ K. Golec-Biernat and M. Wusthoff, Phys. Rev. D 59, 014017, 1999

Color Glass Condensate parametrization (CGC): ¹⁰

$$\begin{aligned}\sigma_{dip} &= 2\pi R^2 N_0 \left(\frac{rQ_s}{2}\right)^{2\{\gamma_s + [\ln(2/rQ_s)/\kappa\lambda \ln(1/x)]\}} & , rQ_s \leq 2 \\ &= 2\pi R^2 \{1 - \exp[-a \ln^2(brQ_s)]\} & , rQ_s > 2\end{aligned}$$

$Q_s = (x_0/x)^{\lambda/2} \text{ GeV} \rightarrow$ saturation scale

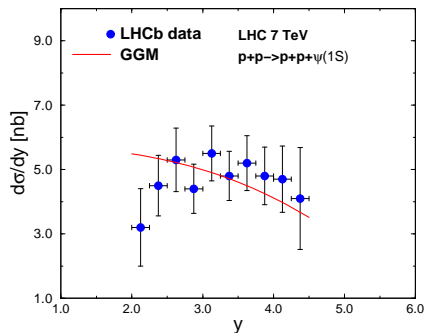
$\gamma_s = 0.63, \kappa = 9.9 \rightarrow$ fixed to their LO BFKL values

$R, x_0, \lambda, N_0 \rightarrow$ free parameters of the fit

$$a = \frac{-N_0\gamma_s^2}{(1-N_0)^2 \ln(1-N_0)}, \quad b = \frac{1}{2}(1-N_0)^{-(1-N_0)/N_0\gamma_s}$$

¹⁰ E. Iancu, K. Itakura and S. Munier, Phys. Lett. B 590, 199, 2004

$\Psi(1S)$ rapidity distribution



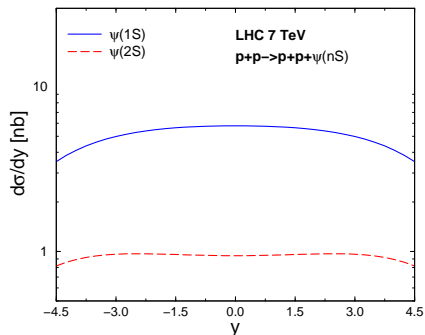
- Predictions to LHC 7 TeV, for pp at forward region ;
- The model CGC was considered for the dipole cross section;
- The relative normalization and overall behavior on rapidity is quite well reproduced in forward regime;
- LHCb data (J. Phys. G 40, 045001, 2013);

Figure: The rapidity distribution of $\Psi(1S)$

photoproduction at $\sqrt{s} = 7 \text{ TeV}$ *

* MBGD, M. T. Griep and M. V. T. Machado, Phys. Rev. D 88, 017504, 2013

$\Psi(1S)$ and $\Psi(2S)$ rapidity distribution



- Predictions to LHC 7 TeV, pp, including mid-rapidity and backward regions ;
- The model CGC was considered for the dipole cross section;
- $\Psi(1S) \rightarrow y = 0: d\sigma/dy \approx 5.8 \text{ nb}$;
- $\Psi(2S) \rightarrow y = 0: d\sigma/dy \approx 0.94 \text{ nb}$.

Figure: The rapidity distribution of $\Psi(1S)$ and $\Psi(2S)$

photoproduction at $\sqrt{s} = 7 \text{ TeV}$ *

* MBGD, M. T. Griep and M. V. T. Machado, Phys. Rev. D 88, 017504, 2013

Our prediction:

$$\sigma_{pp \rightarrow \psi(2S)(\rightarrow \mu^+ \mu^-)}(2.0 < \eta_{\mu^\pm} < 4.5) = 7.7 \text{ pb}$$

LHC measure (J. Phys. G 40, 045001, 2013):

$$\sigma_{pp \rightarrow \psi(2S)(\rightarrow \mu^+ \mu^-)}(2.0 < \eta_{\mu^\pm} < 4.5) = 7.8 \pm 1.6 \text{ pb}$$

Our prediction:

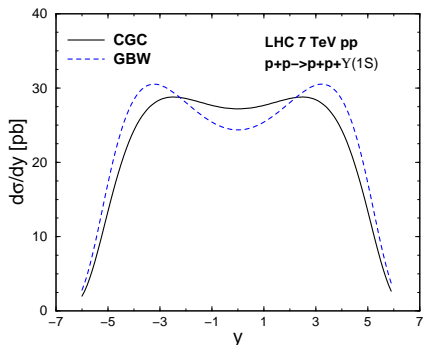
$$[\psi(2S)/\psi(1S)]_{y=0} = 0.16$$

$$[\psi(2S)/\psi(1S)]_{2 < y < 4.5} = 0.18$$

LHCb determination (J. Phys. G 40, 045001, 2013):

$$[\psi(2S)/\psi(1S)](2.0 < \eta_{\mu^\pm} < 4.5) = 0.19 \pm 0.04$$

Differential cross section for Υ production.



- Predictions for LHC 7 TeV, pp ;
- The models CGC and GBW were considered for the dipole cross section;
- Work in progress.

Figure: The rapidity distribution of Υ photoproduction at $\sqrt{s} = 7 \text{ TeV}$.

Coherent process:



\Rightarrow nuclei remain intact.

Incoherent process:



\Rightarrow nuclei are fragmented.

Coherent cross section: ¹¹

$$\sigma^{cohe}(\gamma A \rightarrow J/\psi A) = \int d^2b \left\{ \left| \int d^2r \int dz \Psi_V^*(r, z) \left(1 - \exp \left[-\frac{1}{2} \sigma_{dip}(x, r) T_A(b) \right] \right) \Psi_{\gamma^*}(r, z, Q^2) \right|^2 \right\}$$

$\sigma_{dip} \rightarrow$ dipole cross section.

$\Psi_V \rightarrow$ vector meson wave function.

$\Psi_{\gamma} \rightarrow$ photon wave function.

$T_A(b) = \int dz \rho_A(b, z)$, $\rho_A(b, z) \rightarrow$ nuclear thickness function.

$b \rightarrow$ impact parameter.

¹¹ B. Z. Kopeliovich and B. G. Zakharov, Phys. Rev. D 44, 3466, 1991

Incoherent case: ⁹

$$\sigma^{inc}(\gamma A \rightarrow J/\psi X) = \frac{|Im\mathcal{A}(s, t=0)|^2}{16\pi B_V}$$

where

$$\begin{aligned} |Im\mathcal{A}(s, t=0)|^2 &= \int d^2b T_A(b) \left[\left| \int d^2r \int dz \Psi_V^*(r, z) \sigma_{dip} \right. \right. \\ &\quad \left. \left. \times \exp \left[-\frac{1}{2} \sigma_{dip} T_A(b) \right] \Psi_{\gamma^*}(r, z, Q^2) \right|^2 \right] \end{aligned}$$

$$B_V = 0.6 \times \left(\frac{14}{(Q^2 + M_V^2)^{0.26}} + 1 \right) \rightarrow \text{diffractive slope parameter, } \gamma^* p \rightarrow \psi p$$

$$\frac{d\sigma}{dy}(AA \rightarrow AAV) = \sigma_{\gamma A} \otimes \frac{dN_{\gamma}(\omega)}{d\omega} \quad (10)$$

Photon Flux: ¹²

$$\frac{dN_{\gamma}(\omega)}{d\omega} = \frac{2Z^2\alpha_{em}}{\pi\omega} \left[\xi_R^{AA} K_0(\xi_R^{AA}) K_1(\xi_R^{AA}) \frac{(\xi_R^{AA})^2}{2} K_1^2(\xi_R^{AA}) - K_0^2(\xi_R^{AA}) \right]. \quad (11)$$

$\omega \rightarrow$ photon energy

$K_0(\xi), K_1(\xi) \rightarrow$ modified Bessel functions.

$\xi_R^{AA} = 2R_A\omega/\gamma_L$, $R_A \rightarrow$ nuclei radius.

¹² C. A. Bertulani, S. R. Klein and J. Nystrand, Ann. Rev. Nucl. Part. Sci. 55, 271, 2005

Nuclear shadowing renormalizing the dipole cross section \rightarrow gluon density in nuclei at small Bjorken- x is expected to be suppressed compared to a free nucleon due to interferences.

Ratio of the gluon density: $R_G(x, Q^2 = m_V^2/4)$,¹³

Small- x photon scatters off a large- x gluon or vice-versa.

$\rightarrow y = \pm 3$: x large as 0.02

$\rightarrow y = 0$: $x = M_V e^{\pm y} \sqrt{S_{NN}}$ smaller than 10^{-3} for the nuclear gluon distribution.

¹³ L. Frankfurt, V. Guzey and M. Strikman, Phys. Rept. 512, 255, 2012

Differential cross section for J/ψ production

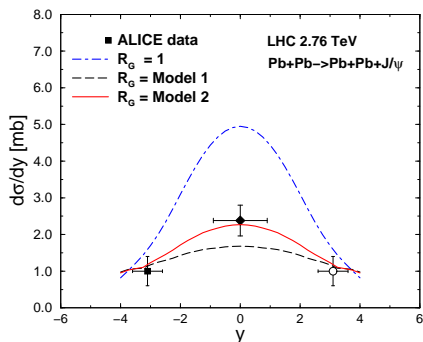


Figure: The rapidity distribution of coherent $\Psi(1S)$ meson photoproduction at $\sqrt{s} = 2.76$ TeV in PbPb collisions at the LHC *

* MBGD, M. T. Griep and M. V. T. Machado, Phys. Rev. C88, 014910, 2013

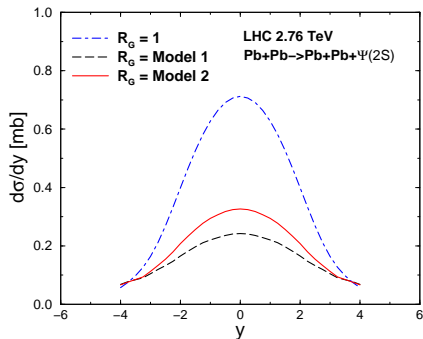
- $\sigma_{dip} \rightarrow R_G(x, Q^2)\sigma_{dip}$;
- R_G Model 1 \rightarrow higher nuclear shadowing;
- R_G Model 2 \rightarrow small nuclear shadowing;
- $R_G = 1$: the ALICE data is overestimate by a factor 2; This prediction is consistent with previous calculations using the same formalism (V. P. Goncalves and M. V. T. Machado, Phys. Rev. C 84, 011902, 2011);
- In the backward/forward rapidity case, the overestimation is already expected as a proper threshold factor for $x \rightarrow 1$ was not included in the present calculation.
- R_G Model 2 is preferred in this analysis.
- ALICE data: Phys. Lett. B718 (2013) 1273 .

Rapidity	$R_G = 1$	R_G Model 1	R_G Model 2
$y = 0$	$d\sigma/dy = 4.95 mb$	$d\sigma/dy = 1.68 mb$	$d\sigma/dy = 2.27 mb$

Table: Results.

- The prediction using Model 2 for R_G describes the ALICE data
- $R_G = 1$ - no shadowing
- R_G Model 1 - decreases 66% and R_G Model 2 - decreases 54% the rapidity distribution compared with $R_G = 1$ (for $y = 0$)
- R_G is considered independent of the impact parameter

Differential cross section for Ψ' production



- R_G Model 1 \rightarrow higher nuclear shadowing;
- R_G Model 2 \rightarrow small nuclear shadowing;
- The theoretical curves follow the same notation as in the $\Psi(1S)$ case;

Figure: The rapidity distribution of coherent $\Psi(2S)$

meson photoproduction at $\sqrt{s} = 2.76$ TeV in PbPb

collisions at the LHC *

* MBGD, M. T. Griep and M. V. T. Machado, Phys. Rev. C88, 014910, 2013,

Rapidity	$R_G = 1$	R_G Model 1	R_G Model 2
$y = 0$	$d\sigma/dy = 0.71mb$	$d\sigma/dy = 0.24mb$	$d\sigma/dy = 0.33mb$

Table: Results.

- $R_G = 1$ - no shadowing
- The theoretical predictions follow the general trend as for the 1S state
- This is the first estimate in the literature for the photoproduction of 2S state in nucleus-nucleus collisions

At central rapidities, the presented predictions give the ratio

$$R_{\psi}^{y=0} = \frac{d\sigma_{\psi(2S)}}{dy} / \frac{d\sigma_{\psi(1S)}}{dy}(y=0) = 0.14$$

→ in the case $R_G = 1$ which is consistent with the ratio measured in CDF¹⁴: 0.14 ± 0.05 (exclusive charmonium production at 1.96 TeV in $p\bar{p}$ collisions)

→ a similar ratio is obtained using Model 1 and Model 2 at central rapidity

→ the ratio is not sensitive to shadowing

¹⁴T. Aaltonen et al (CDF Collaboration), Phys. Rev. Lett. 102, 242001 (2009)

Prediction for the LHC run in PbPb mode at 5.5 TeV:

→ $\Psi(2S)$ cross section ($R_G = 1$):

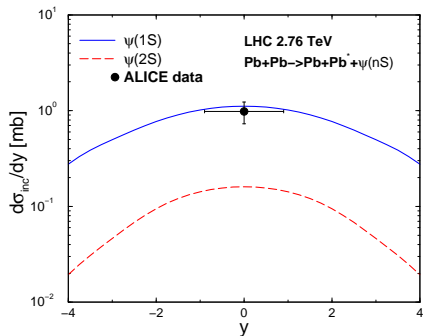
Coherent:

$$\frac{d\sigma_{coh}}{dy}(y = 0) = 1.27 \text{ mb}$$

Incoherent:

$$\frac{d\sigma_{inc}}{dy}(y = 0) = 0.27 \text{ mb}$$

Differential cross section for incoherent J/ψ and Ψ' production.



- Data from ALICE collaboration ;
- The result describes the recent ALICE data for the incoherent cross section at mid-rapidity;
- In both cases we only computed the case for $R_G = 1$;
- ALICE data: Eur. Phys. J.C (2013) 73: 2617.

Figure: The rapidity distribution of incoherent $\Psi(1S)$ (solid line) and $\Psi(2S)$ (dashed line) meson photoproduction at $\sqrt{s} = 2.76$ TeV in PbPb collisions at the LHC *

* MBGD, M. T. Griep and M. V. T. Machado, Phys. Rev. C88, 014910, 2013

$\Psi(1S)$:

$$\frac{d\sigma_{inc}}{dy}(y=0) = 1.1 \text{ mb}$$

$$\frac{d\sigma_{inc}^{ALICE}}{dy}(-0.9 < y < 0.9) = 0.98 \pm 0.25 \text{ mb}$$

→ the prediction describes the recent ALICE data

$\Psi(2S)$:

$$\frac{d\sigma_{inc}}{dy} = 0.16 \text{ mb}$$

→ For the incoherent case, the gluon shadowing is weaker than the coherent case - 20% reduction compared to $R_G = 1$

Differential cross section for Υ production.

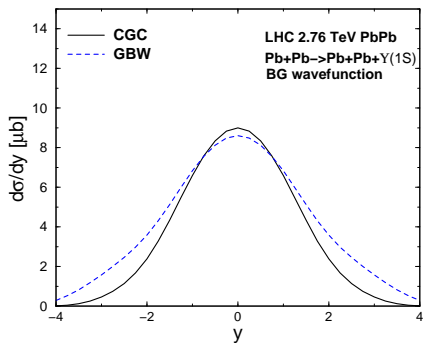


Figure: The rapidity distribution of Υ photoproduction at $\sqrt{s} = 2.76$ TeV.

- Predictions to LHC 2.76 TeV, PbPb ;
- The parametrizations CGC and GBW were considered for the dipole cross section;
- The BG wavefunction was used;
- $y = 0$: $d\sigma/dy \approx 9\mu b \rightarrow$ the two models have approximately equal results in the central rapidity;
- In the forward/backward region, the models presented slightly different results.
- Work in progress.

pp:

The rapidity distributions of mesons $\Psi(1S)$ and $\Psi(2S)$ production were calculated in pp collisions using the dipole formalism.

- The predictions for $\Psi(1S)$ rapidity distribution and total cross section are consistent with LHCb data
- The ratio $\Psi(2S)/\Psi(1S)$ is also consistent with LHCb determination in the forward region
- Our predictions are in agreement with the use of color dipole formalism and with the prediction from Starlight and SuperChic
- Predictions are done also for Υ photoproduction in pp collisions at LHC energies

PbPb:

The rapidity distributions of coherent and incoherent production of mesons $\Psi(1S)$ and $\Psi(2S)$ were calculated in PbPb collisions using the dipole formalism.

- The option of small shadowing is preferred in data description whereas the usual $R_G = 1$ value overestimates the central rapidity cross section by a factor 2, for the coherent case
- The prediction for the state $\Psi(2S)$ photoproduction in PbPb collisions is the first presented in the literature
- The present theoretical approach describes ALICE data for the incoherent cross section
- The central rapidity data measured by the ALICE Collaboration for the rapidity distribution of the $\Psi(1S)$ state is crucial to constrain the nuclear gluon function
- Predictions for Υ photoproduction were presented.

Thank You!